

## Physical-Mechanical Properties of Superhard Nanocomposite Coatings on Base Zr-Ti-Si-N

Alexandr POGREBNJAK<sup>1,2</sup>, Viacheslav BAIDAK<sup>1,2</sup>, Vyacheslav BERESNEV<sup>3</sup>, Petr TURBIN<sup>3</sup>, Nemat MAKHMUDOV<sup>4</sup>, Maxim IL'YASHENKO<sup>1</sup>, Dmitrii KOLESNIKOV<sup>5</sup>, Mannab TASHMETOV<sup>6</sup>

<sup>1</sup> Sumy State University, 40007, R-Korsakov 2, Sumy, Ukraine

<sup>2</sup> Sumy Institute for Surface Modification, PO BOX 163, Sumy, Ukraine

<sup>3</sup> Science Center for Physics and Technology, 61022, pl.Svobody, Kharkov, Ukraine

<sup>4</sup> Samarkand Branch of Tashkent Information Technology University, 2331540, Samarkand, Uzbekistan

<sup>5</sup> Belgorod State University, 308015, Pobeda 85, Belgorod, Russia

<sup>6</sup> Institute of Nuclear Physics, UAS, 100214, Tashkent, Uzbekistan

**crossref** <http://dx.doi.org/10.5755/j01.ms.19.2.4429>

Received 12 January 2012; accepted 28 August 2012

Hard and super hard coatings of Zr-Ti-Si-N of from 2.8  $\mu\text{m}$  to 3.5  $\mu\text{m}$  thickness were fabricated using a vacuum arc source with high frequency stimulation. The samples were annealed in vacuum and in air at 1200 °C. It was found that films with a high Zr and Ti content were thermally stable up to 1180 °C. At the same time, a thin oxide layer of 180 nm to 240 nm was found on the surfaces, which protected the sample from destruction. Below 1000 °C annealing temperature in vacuum, changing of phase composition is determined by appearing of siliconitride crystallites ( $\beta\text{-Si}_3\text{N}_4$ ) with hexagonal crystalline lattice and by formation of  $\text{ZrO}_2$  oxide crystallites. Size of grains of a substitution solid solution (Zr, Ti)N varied from (10–12) nm to 25 nm, but Ti concentration in the solid solution increased. In the process of annealing, hardness of the best series of samples increased from  $(39.6 \pm 1.4)$  GPa to 53.6 GPa, which seemed to indicate that a spinodal segregation along grain interfaces was finished.

**Keywords:** superhard, nanocomposite, compressive stress, spinodal phase segregation.

### 1. INTRODUCTION

Nanocomposite coatings of new generation composed of at least two phases with nanocrystalline and/or amorphous structures are of great interest. Due to very small size (10 nm) of grains and important role of boundary zones surrounding single grains, nanocomposite materials behave unlike traditional materials with grain size higher than 100 nm and display quite different properties. Novel unique physical and functional properties of nanocomposites promote rapid development of the nanocomposite materials [1–5]. Also we should like to note theoretical works [3,4], which studied electron structure, stability, decohesion mechanism, shear of interfaces in superhard and heterostructures nc-TmN/ $\alpha\text{-Si}_3\text{N}_4$ .

The purpose of this work was to study formation of superhard coatings on Zr-Ti-Si-N base and their properties including thermal stability.

These coatings are promising and can be used in engineering for machining machine tools, as well as in areas where durability is an important parameter.

### 2. EXPERIMENTAL

The coatings were fabricated using vacuum-arc deposition (VAD) from the unit-cast, Zr, Zr-Si, and Zr-Ti-Si targets. The films were deposited in nitrogen

atmosphere. The deposition was carried out using standard vacuum-arc and high frequency (HF) discharge methods. Bias potential was applied to the substrate from HF generator, which produced impulses of convergent oscillations with  $\leq 1$  MHz frequency, every impulse duration being 60  $\mu\text{s}$ , their repetition frequency – about 10 kHz. Due to HF diode effect, value of the negative autobias potential occurring on a substrate increased from 2 kV to 3 kV at the beginning of impulse (after start of discharger operation). Coatings of 2  $\mu\text{m}$  to 3.5  $\mu\text{m}$  thickness were deposited on steel substrates (of 20 mm and 30 mm diameter and 3 mm to 5 mm thickness).

**Table 1.** Physical-technological parameters of the deposition

Evaporated materials	Coating	$I_a$ , A	$P_N$ , Pa	$U_{RF}$ , V	$U$ , V	Notes *
Zr	ZrN	110	0.3	–	200	Standard technology VAD
Zr	ZrN	110	0.3	200	–	HF deposition
Zr-Si	(ZrSi)N	110	0.3	200	–	HF deposition
Ti-Zr-Si	(Ti-Zr-Si)N	110	0.3	200	–	HF deposition

\*  $I_a$  is a cathode current in [A];  $P_N$  is pressure of atomic nitrogen in Pa units;  $U_{RF}$  is a bias voltage of HF discharge;  $U$  is bias voltage under conditions of vacuum-arc discharge. The deposition was performed without additional substrate heating. Zr-Ti-Si-N coatings were deposited on poly-crystalline steel (Steel3 – 0.3 wt.%C, Fe the rest). Molecular nitrogen was employed as a reaction gas (Table 1).

\* Corresponding author. Tel.: +380-686-529647; fax: +380-542-334108. E-mail address: [alex@i.ua](mailto:alex@i.ua) (A. Pogrebnjak)

Annealing was performed in air, in a furnace SNOL 8.2/1100 (Kharkov, Ukraine), under temperature  $T = 300\text{ }^{\circ}\text{C}$ ,  $500\text{ }^{\circ}\text{C}$ , and  $800\text{ }^{\circ}\text{C}$ , and in a vacuum furnace SNVE-1.3, under  $5 \cdot 10^{-4}$  Pa pressure, and  $T = 300\text{ }^{\circ}\text{C}$ ,  $500\text{ }^{\circ}\text{C}$ ,  $700\text{ }^{\circ}\text{C}$ ,  $900\text{ }^{\circ}\text{C}$  and  $1180\text{ }^{\circ}\text{C}$ .

Studies of phase composition and structure were performed using X-ray diffraction device DRON-3M, under filtered emission Cu-K $\alpha$ , using secondary beam of a graphite monochromator. Diffraction spectra were taken point-by-point, with a scanning step  $2\theta = 0.05^{\circ}$  to  $0.1^{\circ}$ .

Studies of mechanical characteristics were realized with nanoindentation under 10 nN load of NANOINDENTOR II (MTS System Inc., USA) indentation device with diamond Berkovich pyramid [9].

### 3. EXPERIMENTAL RESULTS AND DISCUSSION

Analyzing phase composition of Zr-Ti-Si-N films, we found that a basic crystalline component of as-deposited on substrate was solid solution (Zr, Ti)N based on cubic lattice of NaCl structure. In Table 2 we present XRD results diffraction: a lattice period in non-stressed cross-section ( $a_0$ ), value of macrodeformation ( $\varepsilon$ ), microdeformation ( $\langle\varepsilon\rangle$ ), and concentration of packing defects ( $\alpha_{\text{def,pack}}$ ). The data were obtained both for the samples after coating deposition and for those annealed in vacuum and air under various temperatures.

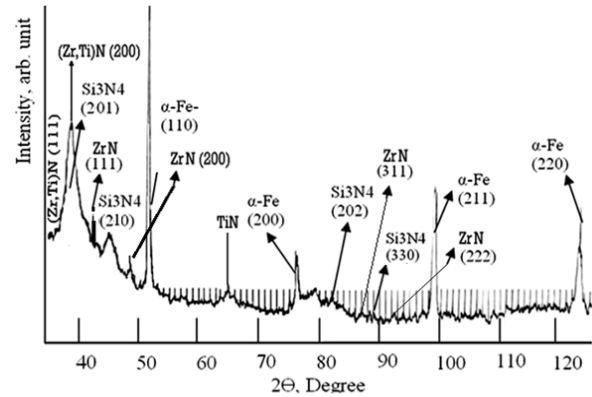
**Table 2.** Changes of structure and substructure parameters occurring in ion-plasma deposited films of Zr-Ti-Si-N system in the course of high-temperature annealing in vacuum and in air

Parameters of structure	After deposition	$T_{\text{an}} = 300\text{ }^{\circ}\text{C}$ vacuum	$T_{\text{an}} = 500\text{ }^{\circ}\text{C}$ vacuum	$T_{\text{an}} = 1100\text{ }^{\circ}\text{C}$ vacuum	$T_{\text{an}} = 300\text{ }^{\circ}\text{C}$ air	$T_{\text{an}} = 500\text{ }^{\circ}\text{C}$ air
$a_0$ , nm	0.45520	0.45226	0.45149	0.45064	0.45315	0.45195
$\varepsilon$ , %	-2.93	-2.40	-1.82	-1.09	-2.15	-1.55
$\langle\varepsilon\rangle$ , %	1.4	1.0	0.85	0.8	0.95	0.88
$\alpha_{\text{def,pack}}$	0.057	0.085	0.107	0.150	0.090	0.128

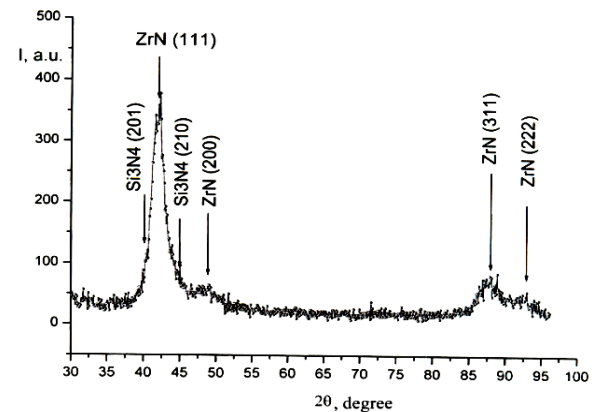
The crystallites of solid (Zr, Ti)N solution underwent compressing elastic macrostresses occurring in a film-substrate system. Compressing stresses, which were present in a plane of growing film, indicate development of compressing deformation in a crystal lattice. It was identified by a shift of diffraction lines in the process of angular surveys ( $\sin 2\psi$  – method) and reached  $-2.93\%$  value (Table 2). With  $E \approx 400$  GPa characteristic elastic modulus and 0.28 Poisson coefficient, deformation value correspond to that occurring under action of compressing stresses. We should also note that such high stresses characterize nitride films, which were formed under deposition with high radiation factor. It also provided high adhesion to the base material due to “atomic peening”-effect.

Qualitative changes of phase composition were observed in films under vacuum annealing at  $T_{\text{an}} > 1000\text{ }^{\circ}\text{C}$ . Appearance of zirconium and titanium

oxides was related to oxidation due to coating surface interaction with oxygen atoms coming from the residual vacuum atmosphere during annealing. At annealing temperatures below  $1000\text{ }^{\circ}\text{C}$ , phase composition of coatings remained practically unchanged (Fig. 1). One could not detect – only changes of width of diffraction lines but their shift to higher diffraction angles as well. The latter characterizes relaxation of compressing stresses in coatings. Changed diffraction lines were related to the increased size of crystallites (in general) and decreased micro-deformation.

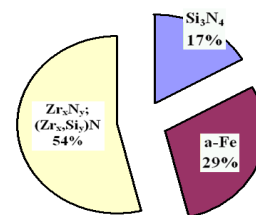


**Fig. 1.** X-ray diffraction pattern of the Zr-Ti-Si-N coatings after deposition



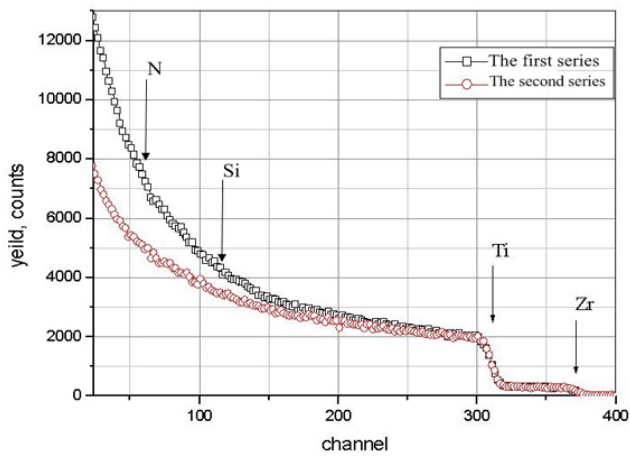
**Fig. 2.** A fragment of diffraction pattern for Zr-Si-N coating deposited by vacuum-arc method with HF stimulation (Fe-K radiation)

Figure 2, shows XRD-diffraction pattern of volume phases for nano-structured Zr-Si-N coating with 10 nm to 12 nm grain sizes for nc-Z $_x$ H phase (where nc is a nano-structured phase).



**Fig. 3.** Histogram of phase ratio for nanocomposite coatings Zr-Si-N

Figure 3 shows the phase relationship, for nanocomposite coating Zr-Ti-Si-N (for Ti $\geq$ 12 wt.%)



**Fig. 4.** Rutherford back-scattering energy spectrum of 1.35 MeV  $\text{He}^+$  ions measured for Zr-Ti-Si-N nanocomposite coating; the arrows indicate kinematical boundaries of elements

Figure 4 shows the results of RBS analysis of the samples coated with Ti-Zr-Si-N. The beam energy of  $^4\text{He}^+$  ions is not sufficient for the analysis of the total film thickness, but the peaks of Ti and Zr are well separated and it can be seen that the concentration of Ti and Zr is almost uniformly distributed over the depth of coating.

But still, Si concentration was not less than 7 at.%, while that of N might reach more than 15 at.%.

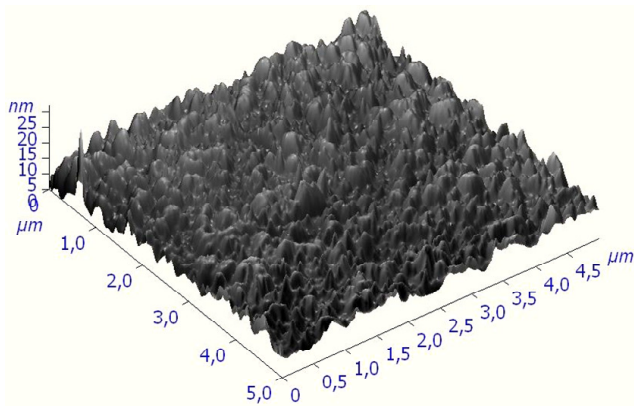


**Fig. 5.** The morphology of surface coatings (Zr-Ti-Si)N after deposition

Figure 5 shows that the surface roughness does not exceed 25 nm. The results are obtained when the parameters of deposition chamber pressure 0.3 Pa, the potential bias applied to the substrate – 200 V.

Mechanical characteristics: the hardness and elastic modulus of nanocomposite coatings Zr-Ti-Si-N before and after annealing are presented in Table 3. It is seen that annealing increases the hardness and elastic modulus.

Upon annealing in air with a temperature 500 °C was much greater hardness, than the samples annealed in vacuum. But annealing in air  $T=300$  °C leads to a decrease in hardness as compared to the base hardness

In Zr-Ti-Si-N coatings, increased Ti concentration, resulted in formation of three phases – (Zr, Ti)N-nc-57 vol.%, TiN-nc-35 vol.%, and  $\alpha\text{-Si}_3\text{N}_4 \geq 7.5$  vol.%, as well as changes of grain size. It decreased to (6 to 8) nm in (Zr, Ti)N and 10 nm to 12 nm in TiN in comparison with the first series. Increase in nanohardness and decrease of

difference in hardness values was observed. Annealing in vacuum below 500 °C finished the process of spinodal segregation at grain boundaries and interfaces. The annealing stimulated segregation processes and formed stable modulated coating structure [1, 5–8].

**Table 3.** The hardness and elastic modulus of nanocomposite coatings (Zr-Ti-Si) N before and after annealing

Mechanical characteristics	After deposition	$T_{am} = 300$ °C vacuum	$T_{am} = 500$ °C vacuum	$T_{am} = 300$ °C air	$T_{am} = 500$ °C air
$H$ , GPa	40,8	43,7	48,6	38,7	55
$E$ , GPa	382	424	456	373	400

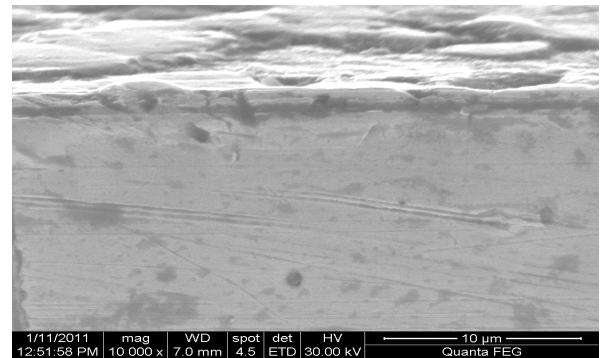


**Fig. 6.** Cross-section of hard coating Zr-Ti-Si-N (high concentration of Si and N)

Figure 6 shows the film cross-section, which demonstrates that in the course of deposition, no cracks were formed and good coating quality was produced. Thickness of the coating was 3.74  $\mu\text{m}$ .

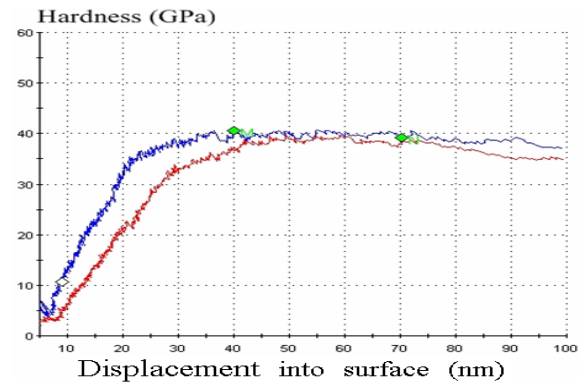


**Fig. 7.** Nano-hardness vs displacement into surface for coatings fabricated using vacuum-arc source with high frequency discharge hardness values for Zr-Ti-N and Zr-Si-N systems

In such a way, hardness, which was increased in the process of annealing, seems to be related to incomplete spinodal phase segregation at grain boundaries resulting from deposition of Zr-Ti-Si-N-(nanocomposite). Annealing stimulated spinodal phase segregation, forming more stable modulated film structures with alternating in volume concentration of phase components (ZrN; (Zr,Ti)N;  $\text{Si}_3\text{N}_4$ ).

Decreased concentration of active oxygen atoms coming from annealing atmosphere increased stability of the film phase composition from 500 °C to 1000 °C.

High macro- and microdeformation occurring in the coating seems to be related to an “atomic peening” effect resulting to non-ordered distribution of titanium atoms implanted to the film during its growth. Highest content of packing defects indicated shift of most closely packed planes in a fcc-sublattice (111) [8–11] and became pronounced under vacuum annealing at  $T_{an} = 800$  °C to 1100 °C reaching 15.5 vol.%.

In Zr-Ti-Si-N coatings, increased Ti concentration resulted in formation of three phases – (Zr, Ti)N-nc-57 vol.%, TiN-nc-35 vol.%, and  $\alpha$ -Si<sub>3</sub>N<sub>4</sub>  $\geq$  7.5 vol.%, as well as changes of grain size, which decreased from 6 nm to 8 nm in (Zr, Ti)N and 10 nm to 12 nm in TiN in comparison with the first series. The annealing stimulated segregation processes and formed stable modulated coating structure [1, 11–13].

#### 4. CONCLUSIONS

The Zr-Ti-Si-N-based superhard nanostructured coatings of different chemical composition were deposited under different growth conditions. An analysis of properties and structure of the coatings was carried out.

It was determined that size of nanograins of solid solution changed from 10 nm to 12 nm. At the same time the size of  $\alpha$ -Si<sub>3</sub>N<sub>4</sub> interlayer, which enveloped the (Ti, Zr)N nanograins, ranged from 6 nm to 8 nm.

The nanohardness varied from 39.6 GPa to 53.6 GPa depending on bias potential on the substrate and pressure in the chamber.

#### Acknowledgments

This work was supported by the GFFR of Ministry Education of Ukraine (Grant F41.1/020 “Development of physical and technological foundations of multicomponent coatings based on Ti-Hf-Si-N; Zr-Ti-Si-N with high hardness >40 GPa, the thermal stability > 1000 °C and high physical-mechanical properties”). The work is also performed in frames of Government contract No 16.552 11 7004 with a financial support of Ministry of Education and Science of Russian Federation.

#### REFERENCES

1. **Pogrebnjak, A. D., Shpak, A. P., Azarenkov, N. A., Beresnev, V. M.** Structures and Properties of Hard and Superhard Nanocomposite Coatings *Uspekhi Fizicheskikh Nauk* 179 (1) 2009: pp.35–64 (in Russian). <http://dx.doi.org/10.3367/UFNr.0179.200901b.0035>
2. **Musil, J., Zeman, P.** Hard a-Si<sub>3</sub>N<sub>4</sub>/MeN<sub>x</sub> Nanocomposite Coatings With High Thermal Stability and High Oxidation Resistance *Solid State Phenomena* 127 2007: pp.31–37.
3. **Beresnev, V. M., Sobol, O. V., Pogrebnjak, A. D., Turbin, P. V., Litovchenko, S. V.** Thermal Stability of the Phase Composition, Structure, and Stressed State of Ion-plasma Condensates in the Zr-Ti-Si-N System *Technical Physics* 55 (6) 2009: pp.871–873 (in Russian). <http://dx.doi.org/10.1134/S1063784210060216>
4. **Veprek, S., Veprek-Heijman, M. G. J., Karvankova, P., Prochazka, J.** Different Approaches to Superhard Coatings and Nanocomposites *Thin Solid Films* 476 2005: pp.1–25.
5. **Musil, J., Dohnal, P., Zeman, P.** Physical Properties and High-Temperature Oxidation Resistance of Sputtered Si<sub>3</sub>N<sub>4</sub>/MoN<sub>x</sub> Nanocomposite Coatings *Vacuum Science and Technology* 23 (4) 2005: pp.1568–1574.
6. **Uglov, V. V., Anishchik, V. M., Zlotski, S. V., Abadias, G., Dub, S. N.** Structural and Mechanical Stability Upon Annealing of Arc-Deposited Ti-Zr-N Coatings *Surface and Coatings Technology* 202 2008: pp. 2394–2398.
7. **Azarenkov, N. A., Beresnev, V. M., Pogrebnjak, A. D.** Structure and Properties of Coatings and Modified Layers of Materials. Kharkovskii Nationalnyi Universitet, Kharkov, 2007: 565 p. (in Russian)
8. **Gavaleiro, A., Hosson, De, J. T.** Nanostructure Coating. Springer-Verlag, 2006: 340 p. <http://dx.doi.org/10.1007/978-0-387-48756-4>
9. **Musil, J.** Physical and Mechanical Properties of Hard Nanocomposite Films Prepared by Reactive Magnetron Sputtering *Nanostructured Coatings, Nanostructure Science and Technology* 2006: pp. 407–463.
10. **Vishniakov, Ja., D.** Sovremennyye Metody Issledovaniia Struktury Deformirovannykh Kristallov. Moscow, Metallurgija. 1975: 480 p. (in Russian).
11. **Sobol, O. V., Pogrebnjak, A. D., Beresnev, V. M.** Effect of the Preparation Conditions on the Phase Composition, Structure, and Mechanical Characteristics of Vacuum Arc Zr-Ti-Si-N Coatings *The Physics of Metals and Metallography* 112 (2) 2011: pp. 188–195 (in Russian). <http://dx.doi.org/10.1134/S0031918X11020268>
12. **Pogrebnjak, A. D., Danilionok, M. M., Uglov, V. V., Erdybaeva, N. K., Kirik, G. V., Dub, S. N., Rusakov, V. S., Shpylenko, A. P., Zukovski, P. V., Tuleushev, Y. Zh.** Nanocomposite Protective Coatings Based on Ti-N-Cr/Ni-Cr-B-Si-Fe, Their Structure and Properties *Vacuum* 83 2009: pp. 235–239.
13. **Pogrebnjak, A. D., Ponomariov, A. G., Shpak, A. P., Kunitskii, Yu. A.** Application of Micro-nanoprobes to the Analysis of Small-size 3D Materials, Nanosystems and Nanoobjects *Uspekhi Fizicheskikh Nauk* 182 (3) 2012: pp. 287–321 (in Russian). <http://dx.doi.org/10.3367/UFNr.0182.201203d.0287>